

FIRE RESISTANCE OF CONCRETE SLABS ACTING IN COMPRESSIVE MEMBRANE ACTION



Tom Molkens¹



Thomas Gernay²



Robby Caspeele³

ABSTRACT

In building renovation, the real behaviour of reinforced concrete slabs cannot always be explained by the bending theory according to classical structural mechanics. Indeed, the bearing capacity, as assessed for instance by a loading test, sometimes appears to be much higher than what would be expected. This phenomenon may be caused by the activation of an arch-effect or so-called compressive membrane action (CMA) which can develop even with small vertical deformations. For a slab which is completely restrained, the presence of reinforcement becomes of lesser importance when this phenomenon is activated (except for end fields). Hence, for fire resistance purposes, it can be discussed whether reinforcement and concrete cover has a smaller influence on the bearing capacity for slabs subjected to fire which exhibit a significant concrete compressive membrane behaviour. This paper presents a loading test performed on a real concrete building which highlighted the development of CMA as the load bearing mode. It then proposes a strategy to evaluate the behaviour resulting from the development of CMA in reinforced concrete slabs at ambient and at elevated temperature based on numerical modelling. The numerical analyses are performed with the finite element software SAFIR[®] using a strip of layered shell elements. A plastic-damage constitutive model with an explicit transient creep formulation is used to capture the concrete behaviour at elevated temperature.

1 INTRODUCTION

In building renovation, it can happen that the bearing capacity of a slab is evaluated as insufficient following the usual bending theory according to classical structural mechanics. Nevertheless, this slab may exhibit a satisfactory behaviour and even, as will be shown in this paper on the basis of in-situ testing, fulfil all requirements even when tested up to the theoretical ultimate limit state load.

¹ Senior project Expert. Building department, Sweco Belgium nv. BELGIUM. e-mail: tom.molkens@swecobelgium.be.
Corresponding Author.

² Postdoctoral Researcher. F.R.S.-FNRS, Structural Engineering Department, University of Liège. BELGIUM. e-mail: thomas.gernay@ulg.ac.be.

³ Professor. Department of Structures for Engineering and Architecture, University of Gent. BELGIUM. e-mail: robby.caspeele@ugent.ac.be.

While the activation of tensile membrane action would lead to excessive deformations incompatible with service conditions and finishing, compressive membrane action (CMA) is the only way to explain the remarkable high capacity of some slabs with limited deformations. However, the question arise as whether this behaviour can also be accounted for in case of a fire below the slab. From a theoretical point of view, the reinforcement is of less importance in such a system, as long as the slab is sufficiently restrained in the horizontal direction. In the present article, the development of compressive membrane action in a slab part of a real structure is studied using thermo-mechanical FEM analysis with the nonlinear finite element software SAFIR® [1]. The Leopold tower project in Brussels is used as case study.

2 COMPRESSIVE MEMBRANE ACTION AT ELEVATED TEMPERATURE

2.1 History and mechanism at ambient temperature

A comprehensive overview of previous research focusing on compressive membrane action (CMA) can be found in [2]. The author stated that a first fundamental basis was published by Ockleston in 1955. It was found that for a restrained slab the load bearing capacity was significantly higher than what could be explained by the yield line theory. However, in order to activate this compressive membrane action, (partly) restrained boundary conditions needed to be implemented at least at two opposite support lines, as shown in *Fig. 1a*. With the recent works of Bailey, which mainly has applications for composite floor slabs with steel decks, most of the attention has been pointed toward tensile membrane action (TMA), which is a highly plastic irreversible effect following CMA, *Fig. 1b*. The direction of the reaction forces are opposite for the two successive systems.

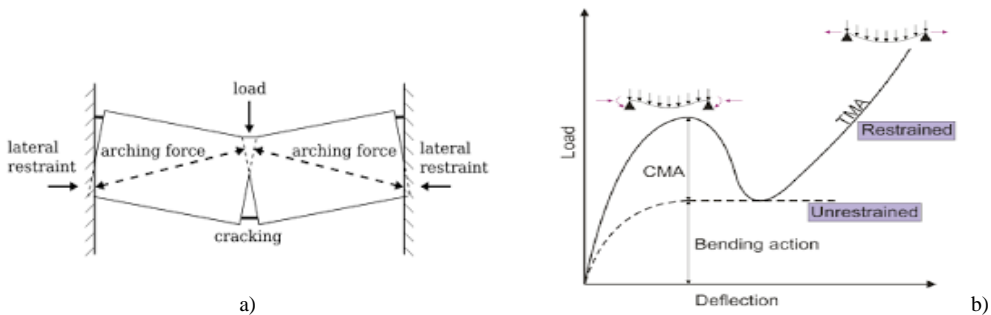


Fig. 1. a) Mechanical system; b) Load-deformation curve for different mechanical systems [3]

2.2 Mechanism at elevated temperature

Due to the increasing temperature at the bottom part of a slab subjected to fire, there will be a loss of mechanical resistance of the concrete. *Fig. 2* shows the isotherms in a slab supported by beams after 7200 sec of exposure to ISO fire. While for bending the central part of the slab is the most critical part, in CMA the slab ends nearby the supports are the most critical. The rise of the arch will decrease due to the weakened concrete at the heated bottom part of the slab.

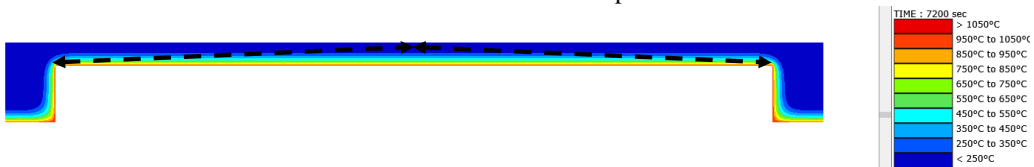


Fig. 2. Typical temperature distribution in a slab supported by beams after 7200 s ISO834 fire

2.3 Analysis by advanced thermo-mechanical analysis

Several FEM-based software tools have been used successfully in the literature to model the development of tensile membrane action (TMA) in reinforced concrete slabs subjected to fire using shell FE (e.g. [4]). However, modelling CMA may be even more challenging in terms of computational robustness, because of the important restraints which block horizontal displacements, and which effects are amplified by the thermal expansion.

In this paper, the development of compressive membrane action in a reinforced concrete slab is analysed using the finite element software SAFIR [1]. The modelling approach consists in representing a 1 m wide strip of the slab, modelled with shell elements positioned on their edge (i.e. the shells are vertical). The model considers different layers over the slab depth, using shells with different time-temperature profiles to account for the non-uniform temperature distribution across the depth (see *Fig. 3*). The time-temperature relationship for a given shell is taken equal to the one of the centre line of the layer as determined from Eurocode (see Section 3.5 for more details). The steel reinforcement was taken into account. The reinforcement was incorporated as uniformly distributed or smeared out only in those shell elements which were located at the appropriate position (i.e., in one horizontal layer of shells located at the position of the lower steel reinforcement and in one layer for the upper reinforcement). A plastic-damage model [5] incorporating an explicit term for transient creep [6] was used as material law for the concrete. The results are presented for the case study in Section 3.5.

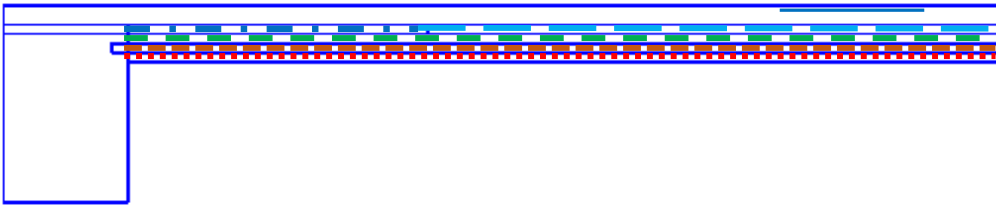


Fig. 3. Shell model of a strip with 5 different temperature layers and reinforcement (lower + upper)

3 CASE STUDY

3.1 Description of the building

An existing concrete building was studied in the framework of its rehabilitation. The investigated building is called the Leopold tower in Brussels; it is a 12-level existing high-rise building with 3 concrete cores without structural joints. Two cores are at the extreme ends and one in the middle which introduces horizontal restraints. In the past, the building was used as an office with an adhesive screed of 60 mm on a slab of 140 mm. The slab span is 5.04 m and the slab is supported by beams (4.42 m distance between beams) of 620 mm wide and 490 mm depth (including the slab thickness). A lower reinforcement of only 335 mm²/m could be measured which is also the upper reinforcement, the latter being curtailed at about 0.75 m distance from the beams. It is the intention to transform the building to apartments. The existing situation is illustrated in *Fig. 4a*.

Several geometrical and mechanical characteristic values were assessed on the basis of on-site inspections and lab tests, $f_{yk} = 400$ MPa, $f_{ck} = 30$ MPa (COV = 7%), $f_{ck, screed} = 15$ MPa (COV = 14%), concrete cover at the bottom is 24 mm (distance to axis) and at the top about 40 mm.

3.2 Test set-up at ambient conditions

As already stated before, the boundary conditions are extremely important when CMA needs to be activated. To verify the behaviour of the slab in ambient conditions a load test set-up was built on site, see *Fig. 5*. The loading test was carried out up to the theoretical ULS-load level equal to 11.58 kN/m². In order to apply this loading, swimming pools were used because they could fit into

the column grid, are easy to fill and the load can be quickly released in case of emergency. Besides the dead loading, which remains present, an additional 7 kN/m² had to be applied (which corresponds to about 80 cm of water). The test set up comprised 4 times 4 swimming pools of 2.2 x 4.4 x 0.84 m³.

During the test, vertical deformations were measured for each step of about 1 kN/m² (additional to the dead load), immediately after increasing the load and again 10 minute later. At the last step the load was kept constant and readings were performed at the time of load application, then after 10, 20 and 30 minutes. No difference was observed in the deflection over these time intervals (the resolution was 0.1 mm with a Leica Sprinter 250M).

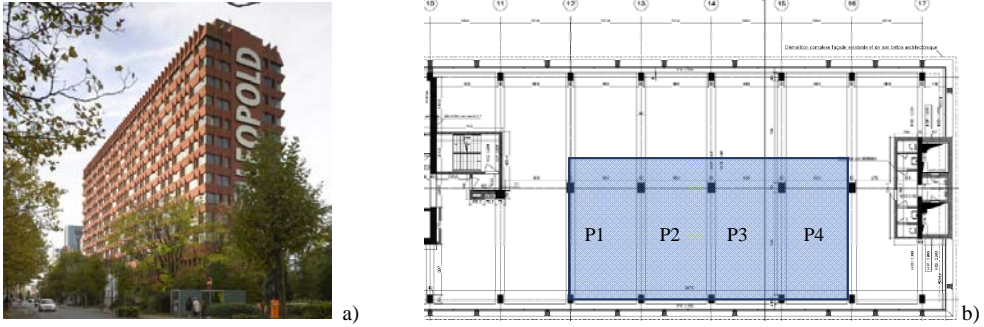


Fig. 4. a) Building before dismantling; b) Floor plan of a typical level and location of the swimming pools used for the loading test.



Fig. 5. Test set-up

3.3 Bearing capacity following elastic and plastic bending theory

At the start of the project an estimation of the bearing capacity was done based on simple elastic bending theory and a rectangular stress diagram in the concrete, as given in Eq. (1).

$$M_{Rd} = (h - c_{centre} - \frac{x}{2})A_s f_{yd} = (h - c_{centre} - \frac{A_s f_{yd}}{2b f_{cd}})A_s f_{yd} \quad (1)$$

where M_{Rd} is the resisting bending moment,
 c_{centre} is the concrete cover (axis distance),
 A_s is the reinforcement area over a width b ,
 f_{yd} is the design yield strength of the reinforcement,
 f_{cd} is the design yield strength of the concrete.

For the positive moments, a resistance of 13.17 kN.m was found and for the negative moments 11.52 kN.m. Together this sums up to 24.37 kN.m at maximum, assuming the best possible

redistribution of forces; in which case the distributed load could be equal to $p_{Ed} \cdot 5.04^2/8$ i.e. $p_{Ed} < 7.68 \text{ kN/m}^2$. This value is much lower than the applied test load (11.58 kN/m^2), which indicates that the observed capacity does not result from bending only. Therefore, it can be assumed that the slab develops CMA.

Actually, considering that the current design (factored) dead load is equal to $4.58 \cdot 1.35 = 6.18 \text{ kN/m}^2$, there would be no reserve in capacity available for any variable load if the slab was working in bending only.

3.4 Numerical FE analysis at ambient temperature

As discussed in Section 3.3., the bending theory cannot explain the capacity observed during the test. The assumption is that CMA develops in the slab. Here, numerical simulations are used as described in Section 2.3 to get a better understanding of the mechanism and to highlight the shift in behaviour from bending to CMA.

A 1 m wide strip of the slab was modelled using stacked shell elements (i.e. layers of shell elements oriented on their edges). In a first approach this model was tested without any reinforcement. The load was again applied in 20 steps. The model (*Fig. 6.*) consists of a half cold beam part at the two ends and a slab part in between. It was assumed that all node displacements and rotations are blocked at the two sides of the model.

Fig. 6 shows the membrane forces in the shell elements. The transition of the bending behaviour (a) to the CMA behaviour (b) can be clearly seen from the distribution of these forces. This transition seems to happen at about 70% of the maximum load level. While in *Fig. 6a* areas which are working in tension and compression are clearly in equilibrium and fill about half of the section, this changes completely after cracking (*Fig. 6b*), where almost the whole section becomes active in compression. Hence, even in the model without reinforcement equilibrium can be found owing to this CMA. Note that the cracks in *Fig. 6b* are in good agreement with those expected in theory and presented in *Fig. 1a*. Looking at the deformed shape in *Fig. 6c*, it is clear that in between the plastic hinges the slabs stays almost straight.

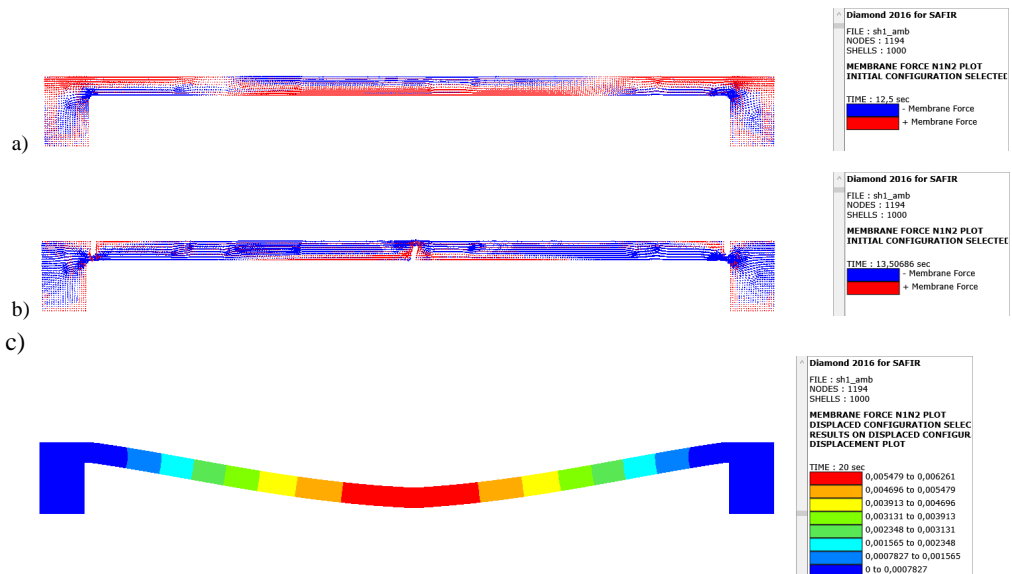


Fig. 6. Principal stresses, blue is compression, red is tension, a) working in bending, b) working in CMA, and (c) deflected shape amplified 50 times at full test load (ULS).

In Fig. 7, the numerical results obtained with SAFIR without reinforcement (dotted line) are compared to the test results. Note that the starting points (reference) for the measurements are the calculated deformation at the load level due to the dead loads. According to the measurements there is no clear transition zone between bending and CMA behaviour, whereas the FEM analysis clearly illustrates such a transition. This could be due to the lower and upper reinforcement which make the transition not so abrupt in reality, whereas this reinforcement has not been included in the model.

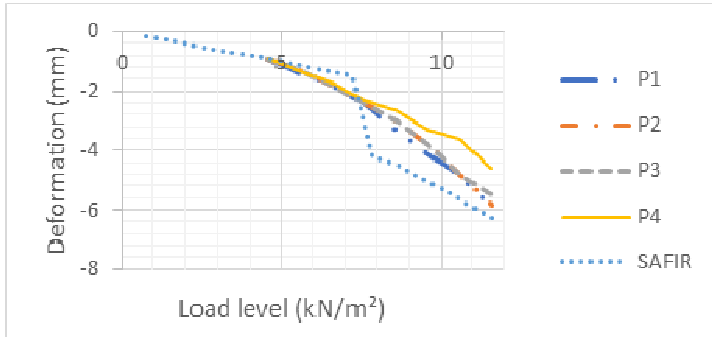


Fig. 7. Load-deformation curve for reference points: comparison between test results and SAFIR.

3.5 Numerical FE analysis at elevated temperature

Next, the fire resistance of the slab has been studied. Several fire simulations were performed with the 1 m strip multi-layer shell model, where each layer is assigned a different temperature profile as presented in Fig 3. Also, the reinforcement was included in the model as explained in Section 2.3. Over the depth of the slab, 6 layers of elements were used with a depth of $140/6 = 23.33$ mm each. The temperature in the four bottom layers (1 till 4) reaches significantly high values which reduce the concrete strength. For the simulations, the temperature at mid-height of the different layers are considered in the numerical model. These time-dependent temperature profiles are taken in accordance to figure A2 of EC2-1-2 [7], as shown in Fig. 8. The temperatures in the two top layers (5 and 6) remains below about 100 °C and hence do not significantly affect the compression resistance. As such, a constant temperature (20°C) is assumed for these layers in the model. The applied load on the slab is reduced to 8.08 kN/m², which is equal to the design load in case of fire.

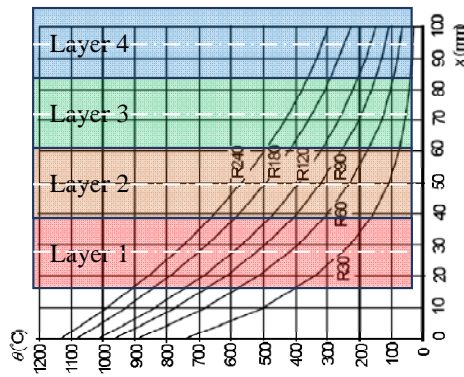


Fig. 8. Time dependant temperature profiles of different layers

The simulation in fire situation ended after 29 minutes. It is interesting to observe the distribution of membrane forces at the time when the simulation stops (*Fig. 9*) and to compare with the results presented in *Fig. 6(b)*, corresponding to the ultimate load at ambient temperature. Based on *Fig. 9* it can be seen that cracks are appearing a little bit shifted away from the sides of the beams, while the upper layer above the reinforcement is still working in tension. The behaviour is also affected by the thermal gradients, since the upper layers remain colder than the lower layers. It seems also that the slab part is disconnecting from the lower beam part, in practice however transverse reinforcement of the beam will avoid this effect.

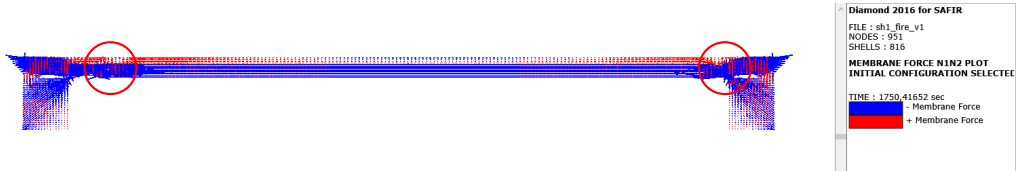


Fig. 9. Principal stresses at failure time for an unprotected slab

The fire resistance can be increased by adding a protection layer to reduce the temperatures in the slab. To study the effect of thermal protection, three additional calculations were performed, each with a shift of the temperature profiles attributed to the layers with one step to the bottom. As the concrete slab is foreseen from an insulation material thickness equal to the effect of one, two or three concrete layers of 23.33 mm. The obtained fire resistance (*R*) is illustrated in *Fig. 10 a* as a function of the surface temperature of the layer.

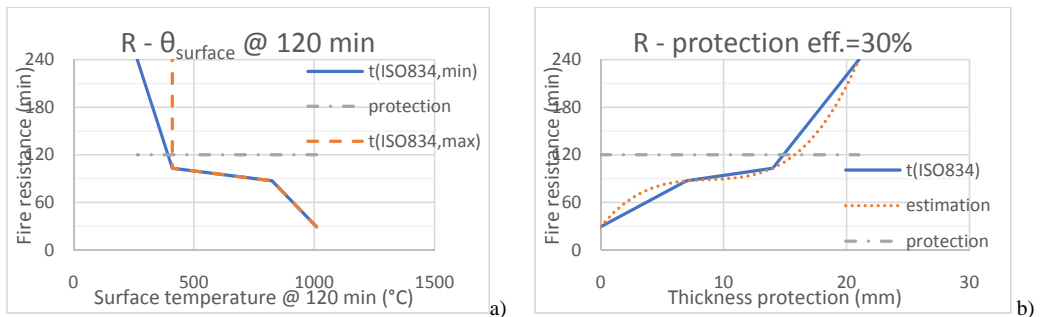


Fig. 10. a) *R* in function of surface temperature @ 120 min; b) *R* in function of equivalent insulation thickness

With a bottom layer characterised with a surface temperature of maximum 265 °C after 120 minutes (or a mean temperature of 210 °C @ 120 or also 370°C @ 240 minutes) no failure could be obtained, even not after 240 minutes. As lower boundary, the solid line of *Fig. 10a* can be used, and the dashed one as upper boundary. To obtain a fire resistance of 120 minutes (which is required in this case), the surface temperature must be limited to 383 °C.

Another way to approach the problem is by supposing an insulation layer with for example an efficiency of 30% in the meaning that only $0.30 \cdot 23.33 = 7$ mm of insulation material achieves the same effect as one layer of 23.33 mm concrete in our model. This is plotted in *Fig. 10b* together with a cubic regression line, which results in 16 mm of insulation material. The failure times corresponding to 7, 14 and 21 mm of insulation are respectively 87, 103 and > 240 minutes.

4 CONCLUSIONS

Compressive membrane action can play a major role in restrained structures. Using advanced numerical analyses with suitable material models, this phenomenon can be simulated at ambient temperature showing a distribution of forces and cracks in line with theory. Furthermore, a reasonable agreement has been found with a loading test performed on a real multi-story concrete structure in terms of vertical deflection.

Modelling of compressive membrane action at elevated temperature is challenging, in part due to the important restraint forces that build up in the model. Nevertheless, the obtained results have shown that advanced analyses can be used to derive the maximum surface temperature and/or insulation thickness for a required fire resistance. Additional works will be conducted to refine the models at elevated temperature, for instance analysing the minimum number of layers that should be used across the depth to capture properly the effects of thermal gradients.

REFERENCES

- [1] Franssen J.M. (2005). *SAFIR A Thermal/Structural Program for Modelling structures under Fire*, Engineering Journal A.I.S.C. 42(3): 143-158.
- [2] Gourverneur D. (2014). *Experimental and numerical analysis of tensile membrane action in reinforced concrete slabs in the framework of structural robustness*. Phd thesis, U Gent, Belgium.
- [3] Wouter B., Caspee R., Gourverneur D., Taerwe L. (2014). *Influence of membrane action on robustness indicators and a global resistance factor design*. IABMAS 2014 - Bridge Maintenance, Safety, Management and Life Extension, Shanghai.
- [4] Vassart, O., et al. (2012). Large-scale fire test of unprotected cellular beam acting in membrane action. *Proceedings of the Institution of Civil Engineers: Structures and Buildings* 165 (7): 327-334.
- [5] Gernay T., Millard A., Franssen J.M. (2013). A multiaxial constitutive model for concrete in the fire situation: Theoretical formulation. *International Journal of Solids and Structures* 50(22-23): 3659-3673.
- [6] Gernay T., Franssen J.-M. (2012). *A formulation of the Eurocode 2 concrete model at elevated temperature that includes an explicit term for transient creep*. Fire Safety Journal 51: 1-9.
- [7] EN 1992-1-2 (2004+AC2008). *Eurocode 2: Design of concrete structures – Part 1-2: General rules – Structural fire design (+AC2008)*. CEN, Brussels, Belgium, December 2004.